2024 IEEE International Conference on Robotics and Automation (ICRA 2024)
May 13-17, 2024. Yokohama, Japan

OriTrack: A Small, 3 Degree-of-Freedom, Origami Solar Tracker

Crystal E. Winston*[1,2] and Leo F. Casey[2]

***Abstract*—In response to the need for sustainable energy solutions, solar panels have gained significant traction. One way to increase the energy capture of solar systems is through solar tracking, a means of reorienting solar panels throughout the day in order to face the sun. The energy consumption increase that comes with solar tracking often far outweighs the amount of energy required to move the panel, which makes it a compelling strategy for improving solar systems. Unfortunately, while solar trackers are commonly used in large solar farms, they are rarely used on rooftops, an area where solar panels are commonly installed. This is for two primary reasons: (1) most commercially available solar trackers are too large to be installed on roofs and (2) even if traditional solar trackers were made in a more compact form-factor it would be difficult to densely lay them out on a roof without the trackers substantially shading each other. In order to address these issues, we introduce OriTrack, a small three-degree-of-freedom (3 DOF) solar tracker which reduces the area of its shadow by reducing its height as it tracks the sun. In this paper we discuss the design, manufacturing, and control of OriTrack. We then compare OriTrack to a flat reference panel, the solar energy solution commonly used on roofs today, and find that OriTrack demonstrates 23% increased energy production. This result suggests OriTrack could be used as a future solution for solar tracking on rooftops.**

***Index Terms*—Energy and Environment-Aware Automation, Soft Robot Applications, Soft Robot Materials and Design**

I. Introduction

In recent decades, the world has experienced a rapid change in climate patterns, driven primarily by the increase in anthropogenic greenhouse gas emissions [1]. The alarming consequences of climate change have underscored the urgent need to transition away from fossil fuels towards cleaner and more sustainable sources of energy [1], [2]. In light of this, renewable energy technologies have emerged as vital tools for mitigating the effects of climate change and fostering a sustainable energy future.

Solar energy, as a prominent renewable resource, can meet a substantial portion of the world's clean energy demands because it produces negligible greenhouse gases [3]. However, the efficiency of solar energy conversion is significantly influenced by the angle of incidence of sunlight on solar panels [4]. For this reason, solar tracking has gained traction. Solar trackers dynamically adjust the orientation of solar panels to directly face the sun throughout the day. This dynamic adjustment enhances energy capture by maximizing the absorption of solar radiation [5]. While solar trackers are commonly used in large solar farms, they are almost never used on roofs, even though installing solar panels on roofs is becoming an increasingly common practice. This is because commercially available solar trackers are too large to be installed on most roofs and the shadows that they produce also make it so that they cannot be densely packed together in a confined area. In this work, we address these issues by designing a solar tracking system better suited for roofing applications.

Solar trackers come in single-axis and dual-axis configurations. The former follows the sun's east-west path, while the latter also makes small adjustments to the panel's north-south orientation which is known to further increase energy capture [6], [7]. The vast majority of active dual-axis solar trackers consist of a mast that is connected to the solar panel through a motorized pan-tilt mechanism [5], [7]. A lot of solar tracking research focuses sun angle sensing and control strategies [8]–[12]. However some work has been done on the mechanical design of these trackers, with the aim of either reducing cost [13], investigating mechanisms for actuating multiple panels [14], or investigating novel mechanism designs [15], [16].

When used in a large solar farm, these trackers are typically installed in rows with substantial space between them in order to mitigate the effects of solar trackers casting shadows on the panels behind them. Optimal layouts vary based on total area available and location of the solar farm, but a typical optimized solar farm with pan-tilt based dual-axis trackers can have layouts where less than 50% of the total occupied area actually contains solar panels [17]. In order to mitigate the effects of self-shading, we have developed a three-degree-of-freedom (3 DOF) solar tracker that also varies its height as it tracks the sun, thus reducing the shadow it casts and allowing for a more densely packed array.

OriTrack uses an origami-inspired structure that allows it to track the east-west and north-south movements of the sun. This structure is different from the traditional pan-tilt mechanism used in the majority of dual-axis trackers because it allows the solar tracker to also reduce its height throughout its tracking trajectory within a relatively compact and easy to manufacture form factor. This reduces the shadow cast on neighboring trackers. OriTrack is also much smaller than a typical solar tracker, with a single solar cell that is 125mm x 125mm. For reference, a typical solar tracker moves a panel with hundreds of solar cells of this size, and has a total surface area between 30m^2 - 40m^2 [18]. This size reduction allows it to be more easily installed on roofs. Fig. 1a shows

*cwinston@stanford.edu
[1] Department of Mechanical Engineering, Stanford University, CA 94305, USA
[2] Google X, Mountain View, CA 94043, USA

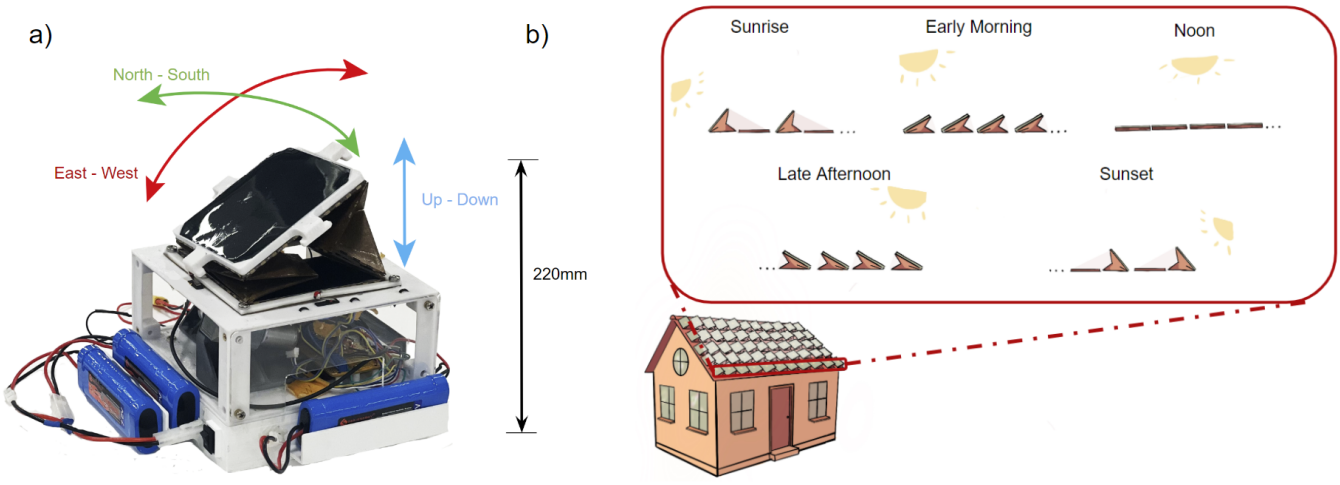

Figure 1. **a)** A single OriTrack with its degrees of freedom labeled. The height of the structure in this configuration is 220 *mm*, which is shown as a reference for scale. **b)** This illustration shows a potential layout for multiple OriTracks on a roof. In this implementation, the OriTracks are tightly packed together. At sunrise and sun set, only half of the trackers are actively tracking the sun. Throughout the remainder of the day, from early morning, to late afternoon, the height of each tracker is reduced and the shadow cast is substantially smaller. During that time, all of the OriTracks are actively tracking the sun.

an image of OriTrack with its degrees of freedom and Fig. 1b shows an illustration showing how it could be laid out in a densely packed array. As shown in Fig. 1b, on any given day, certain cells in the solar array could be actively tracking the sun from sunrise to sunset while others could act as passive, flat panels in the early morning and late evening, when they are likely to be in the shadow of neighboring trackers and be used as active trackers for the majority of the day when shadows cast on them are small or non-existent. This is possible because as the sun gets closer to it's highest point in it's daily trajectory, the active trackers will decrease their height, thus reducing the shadows cast on neighboring cells. The trackers that are active or passive for all or part of the day could vary from day to day depending on the sun's trajectory.

This paper discusses the design, manufacturing, control, and testing of a single, 3 DOF solar tracker, called an OriTrack, that could be used in this larger solar tracking array. The OriTrack was tested from sunrise to sunset on September 8, 2023 in Mountain View California and produced 23% more energy when compared to a flat reference panel.

II. Design, Manufacturing, Kinematics, and Shading

A. Origami Structure Design, Fabrication, and Actuation

This solar tracker uses a 3 DOF structure that has two angular degrees of freedom as well as a change in height, as depicted in Fig. 1a. It uses a water-bomb base on each of its four sides, which is an origami structure that produces a spherical joint [19]. When each water-bomb base is placed on the parallel structure shown in Fig. 2b, it results in these three degrees of freedom and can take on either a kink-in or kink-out configuration. Similar origami structures have been used for a variety of applications ranging from haptic devices [20], [21], to surgical grippers [22], to collapsible manipulators [23]. Although this particular structure has four spherical joints, only three of them must be actuated in order to control its three degrees of freedom [24]. The fourth spherical joint is allowed to move passively so as not to over constrain the system. We chose to actuate the two joints along the east-west axis, and one joint along the north-south axis. However, any set of three actuated joints should produce the same workspace.

The origami structure on OriTrack was made from a 1.2*mm* thick laser cut sheet of chipboard. The chipboard was cut with an Epilog Laser Fusion 60*W* CO_2 laser cutter into the pattern shown in Fig. 2a. The dashed hinges were then scored with a razor blade so that each hinge could only bend 180°. If one tries to bend the joint such that it opens the scored line, the hinge bends easily. However, if one tries to bend it in the opposing direction, it does not bend until the hinge is ripped. The straight and diagonal lines in the cutout pattern were scored on opposing sides of the chipboard sheet, as depicted in Fig. 2a. This is so that those hinges bend in opposing directions. This forces the structure into a kink-in, rather than kink-out configuration, allowing the individual solar trackers to be packed more closely together when laid out in a solar tracking array. Each of the hinges were then reinforced with Eclectic E6000 Craft Adhesive, a flexible adhesive that was used to prevent the joints from tearing due to extended use. The entire sheet was then coated in six thin layers of Shellac on each side to help stiffen the structure, and 0.5*mm* spring steel cutouts were adhered to the trapezoidal faces where

the actuators push and pull on the water-bomb joints. These spring steel reinforcements help mitigate any deformation caused by large forces exerted on those faces. On the opposite side of the sheet, tabs that allow the structure to attach to actuators and plates that allow the solar cell to be screwed to the top face of the origami structure were adhered. This sheet was then folded and adhered to a chipboard and acrylic plate that allowed it to be screwed to a 3D printed base. A solar cell holder was 3D printed from white polycarbonate, and heat set inserts were inserted in the back of that holder, so that it could be screwed onto the origami structure. A 3.6W C60 SunPower solar cell was then sealed into the holder with Kisrel epoxy resin, and wires were soldered to the positive and negative pads on the back of the cell and routed through the holder. The solar cell and holder assembly was then screwed onto the origami structure and the solar cell wires were routed through a hole in the top of the origami structure and they then exit the solar tracker through the 3D printed base.

The 3D printed base holds JGY-370 motor assemblies which consist of a brushed DC motor, encoder, and worm gear box. These motors drive three of the waterbomb joints in the structure. Although the structure has four water-bomb joints, only three must be actively controlled in order to control the height and orientation of the solar panel [24]. The worm drive motors actuate the water-bomb joints through linkages as shown in Fig. 3. Worm drive motors were used because they are non-backdrivable. This allows for certain trackers to act as passive flat panels at times when it is advantageous to do so, like during a windy storm or when they are in the shadow of neighboring trackers at sunrise and sunset. The non-backdrivable gear train on these motors allows the structure to remain flat without the need to expend energy to hold it in that configuration. It also allows OriTrack to maintain a set angle while it is tracking without providing power to the motors.

The encoders mounted to each motor provide feedback for controlling its angle. At the start of each day, the tracker goes through a zeroing sequence where all three motors are used to lower the solar cell. When the cell is level with the ground and at its lowest height, tabs on the solar panel holder contact limit switches on the base. When these limit switches are hit, the angle for each water-bomb base is set to zero. This is done to account for backlash in the drive train and compliance in the origami structure that may lead to a decrease in accurate estimate of the water-base joint angle over time.

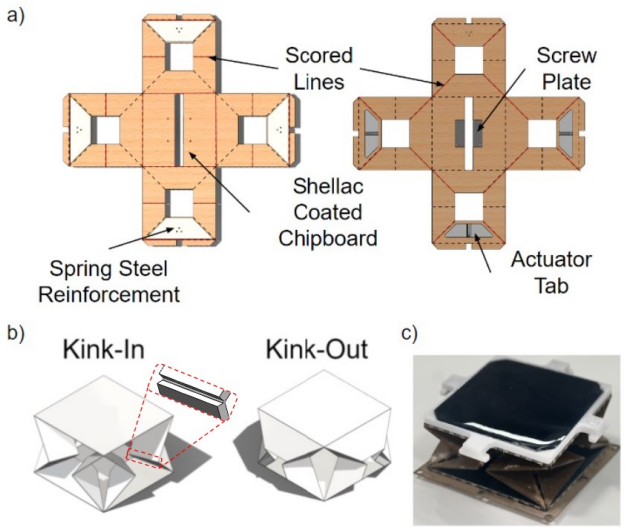

Figure 2. **a)** This image shows the flat origami structure before it is folded. The red lines denote which hinges are scored with a razor blade after laser cutting. This scoring is what forces the structure into a kink-in configuration. **b)** This image shows the distinction between the kink-in and kink-out configurations that the origami structure can take. Scoring the joints is what forces the structure into a kink-in configuration. A cross section of the shape of this joint is shown in the kink-in image. **c)** This is an image of the finished origami structure with solar cell added before it is attached to the base containing OriTrack's actuators.

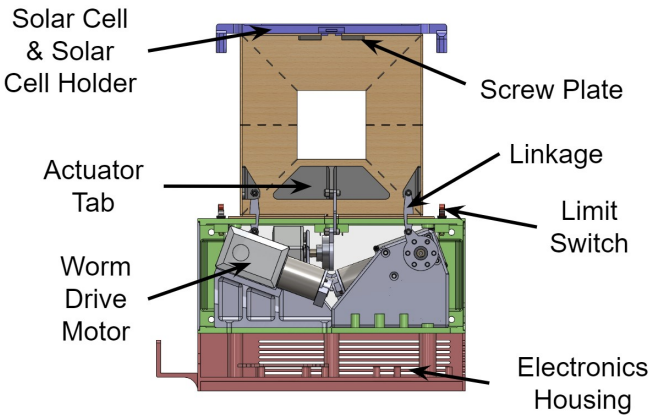

Figure 3. This image shows a cross section view of OriTrack. It shows how the linkages connect from the origami structure to the worm drive motors, and also labels critical parts of the system.

B. Kinematics and Control

The azimuth and zenith angles of the sun can be calculated for any given date, time, and location. We used the sun tracking algorithm developed by Blanco et al. to calculate the position of the sun, and this allows us to schedule the trajectory of the 3 motors for any given day. This algorithm has an average sun angular error of 8.78 arcsec (0.002°) over the years 2020-2050 [25]. After completing the zeroing sequence, the tracker starts its trajectory by moving to face the sun at sunrise. Once it reaches its first set-point, the system goes into a low power mode where the motors, encoders, and motor drivers are turned off and the micro controller turns off its digital pins. In this low power mode, a real time clock is running to determine when to exit this mode and move to the next set-point. The system changes its desired set point every 10 minutes and exits the low power mode when the desired set point changes. This 10 minute interval was chosen based on our observation that OriTrack

takes on average 30 seconds to reach a desired set point. By choosing to change the desired setpoint every 10 minutes, it is in a low power mode 95% of the time, making it easy to conserve energy. However, more investigation could be done on this timing scheme which considers the rate at which the sun's angular position changes throughout the day and how much energy is lost by being misaligned until OriTrack reaches the next set point. We discuss investigating this more in Section IV.

Each of these set-points is represented using the coordinate system shown in Fig. 4. In this figure, the vector $\vec{r}$ points from the origin to the center of the solar cell. The angle δ represents the angle from the z axis to $\vec{r}$. θ represents the angle between the projection of $\vec{r}$ into the x-y plane and the x axis, which points east. Conversions between θ and δ to azimuth and zenith angles are given in Eq. (1) and Eq. (2).

$$\theta = Zenith \tag{1}$$

$$\delta = Azimuth - 90^\circ \tag{2}$$

Using the kinematics in [24], we plotted the workspace for the device as shown in Fig. 5. In this plot, the x, y, and z values are normalized by r_a which is half the side length of the square face on the origami structure that the solar cell is mounted to. We then identified the points shown in red in Fig. 5, as the smallest heights the device could reach for a given set of δ and θ, i.e. the points that minimized z. For each minimum height point in the workspace we then calculated the joint angles, α_i, using the formulas given in [24] and used that to generate a lookup table mapping minimum height positions to joint angles. This lookup table has a δ and θ step size of 1.2 °. From there, we then interpolated within the lookup table to produce a set of angle commands, which vary every ten minutes, for a given date and location. These commands were then uploaded to OriTrack's micro controller.

In order to reach each set point, a PID controller computed the control signal for each motor based on feedback from the motor's encoder. The control loop for reaching different set points is given in Fig. 6.

C. Shade Reduction

Using the same kinematic model discussed in Section II-B, we also estimated the shadow cast by OriTrack outside of its footprint and compared this to traditional dual-axis solar tracker with a mast. We did this calculation for September 8, 2023 in Mountain View California, the time and location of the outdoor test discussed in Section III. In this calculation we assumed both OriTrack and and the dual axis tracker have the same angular workspace, meaning they can reach all the same values of δ and θ. We also assume both trackers track the sun in 10 minute increments and that the mast of the dual axis tracker is the minimum possible height that allows it to have the same angular workspace as OriTrack. While

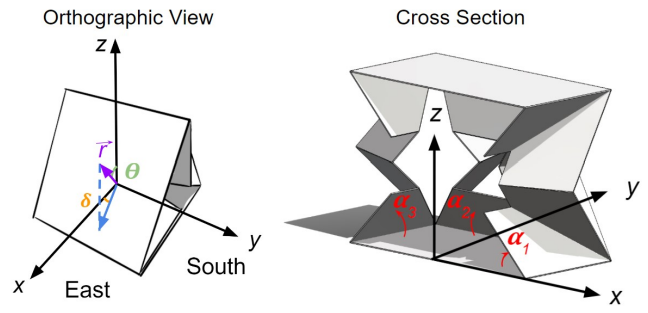

Figure 4. This figure shows the coordinate system used to describe the kinematics of the system.

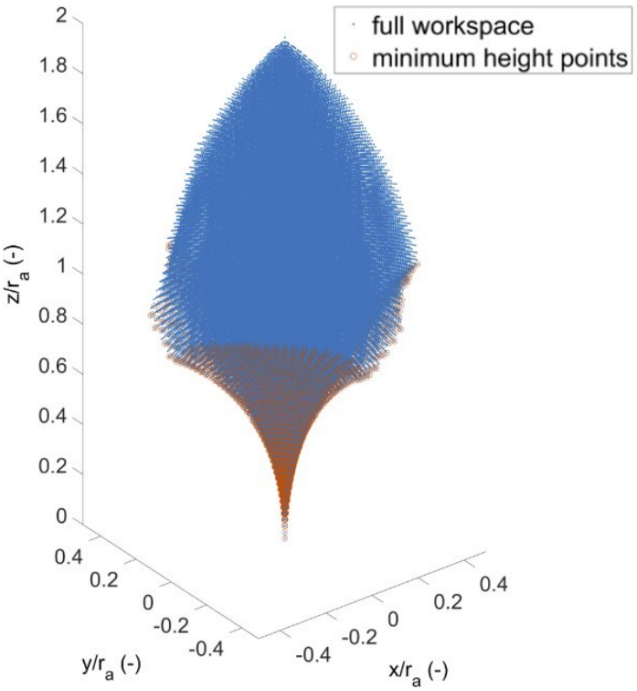

Figure 5. This plot shows the workspace for the structure, as presented by [24]. The blue points show all possible points that could be reached by the vector $\vec{r}$ in Fig. 4. In this plot, all axes are normalized by r_a, which is half the side length of the central square on the origami structure that the solar panel is mounted to. The red points show all points with unique δ and θ with minimum value of $\frac{z}{r_a}$.

the sun was within the workspace of both trackers, OriTrack produced a shadow that was 21% smaller than a traditional mast design, which suggests this origami based design would allow for a more densely packed array of trackers than a mast design. A plot of both shadows is shown in Fig. 7.

III. Results and Discussion

In order to test the system, OriTrack operated outside on September 8, 2023 in Mountain View California from sunrise to sunset, which was 6:44am to 7:26pm PST. A flat reference panel was also laid outside next to OriTrack

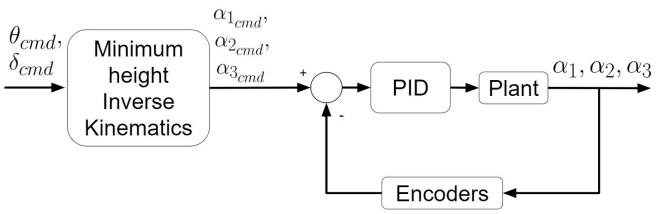

Figure 6. This control loop is used to control the angle of each motor on OriTrack. The desired θ_{cmd} and δ_{cmd} change every 10 minutes based on the time of day and are fed into the minimum height inverse kinematics. From those inverse kinematics, we find $\alpha_{1_{cmd}}$, $\alpha_{2_{cmd}}$, and $\alpha_{3_{cmd}}$ and feed that into a PID controller that uses the encoders mounted to the motors as feedback.

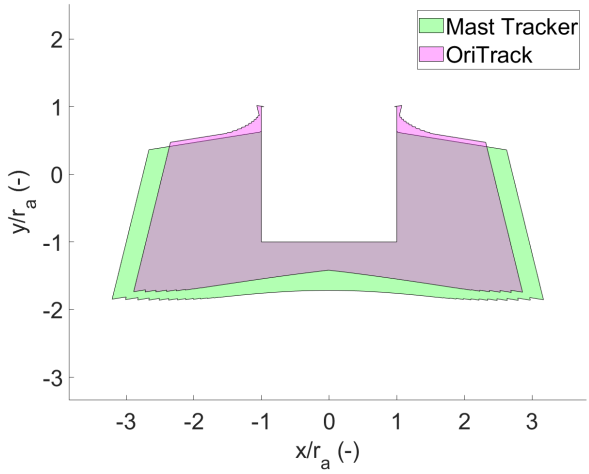

Figure 7. A plot showing the estimated shadow cast by OriTrack and a traditional dual-axis mast solar tracker when the sun is within the solar tracker's workspace. OriTrack's shadow is 21% smaller than that of the traditional dual-axis tracker.

for comparison. This comparison aims to demonstrate that OriTrack can capture more energy than the flat panels commonly used on roofs today and thus works as a viable solar tracking solution. OriTrack's solar cell was connected to a $50W$ 0.1Ω power resistor and a DATAQ DI-808 data logger was used to measure the voltage drop across the resistor at $0.05Hz$ throughout the experiment. A 0.1Ω power resistor was selected based on current and voltage produced by the solar panel at the maximum power point provided in the solar cell datasheet [26]. An identical solar cell, which was placed in the same solar cell holder and coated in the same epoxy resin as the solar cell on the OriTrack, was laid flat next to the tracker and was connected to a different $50W$ $0.1\ \Omega$ power resistor as a reference. The voltage drop across the flat panel's resistor was measured by a separate channel on the data logger. These circuits are depicted in Fig. 8. Power output was then calculated using the measured voltages and known resistor value, and that power data was then numerically integrated over the length of the experiment to estimate the total energy captured that day. A Peacefair PZEM-031 power meter was also attached to the circuit driving the solar tracker's electronics in order to measure how much energy was consumed by the motors, micro controller, encoders, and real time clock.

When accounting for the amount of energy required to operate the system, the solar tracker produced 23% more energy at the end of the test when compared to the flat reference panel. This is comparable to other dual-axis solar trackers [5], [6]. The amount of energy produced on any given day would be expected to vary based on temperature, location, and cloud conditions, but this test does demonstrate promising results towards the use of such a solar tracker in a larger array mounted to a rooftop.

In addition to measuring the energy captured by the solar tracker throughout the day, we also attached an OpenLog Artemis data logger with a built in ICM-20948 9DOF IMU to the underside of the solar panel in order to estimate the solar cell's orientation throughout the experiment and assess the tracking accuracy. In order to do this, we used the MATLAB ecompass algorithm, which estimates orientation of the IMU based on magnetic north and accelerometer readings.

A plot showing the desired and measured solar panel angles is shown in Fig. 9. Throughout the course of the experiment there was an RMSE of 8.2° for θ and an RMSE of 29.2° for δ. In this experiment, OriTrack followed the general trajectory shape of θ commands with an offset of 8°. However in δ, it follows a trajectory of a different shape. We believe both of these tracking errors are predominantly the result of compliance in the origami structure which is not accounted for in the kinematic model. We would like to stiffen the unhinged portions of OriTrack's structure in order to further investigate this, which we discuss in Section IV. Backlash in the system and errors in reaching each setpoint, are also factors. However, the largest angular error for any individual motor throughout the course of the experiment was only 2.7° and the backlash in any individual motor and linkage subassembly is at most 3.5°. While the energetic gains of this system are certainly substantial, some dual axis solar trackers have been shown to produce over 40% more energy when compared to a flat panel [5]. Improving this tracking accuracy would allow OriTrack to produce even greater energetic gains, while minimizing shading, which will be the focus of our future work.

IV. Conclusion and Future Work

In this paper, we discussed the design, manufacturing, and testing of OriTrack, a 3 DOF, origami-inspired, solar tracker. The tracker has two angular degrees of freedom, and can also adjust its height in order to reduce the shadow it casts on nearby solar trackers in the array. Each OriTrack in an array increases energy production at the cell level by tracking the sun. Furthermore, the ability for each OriTrack to also adjust its height also enables increased spacial efficiency of an array of OriTracks, as individual trackers can be installed more closely together without producing shadows

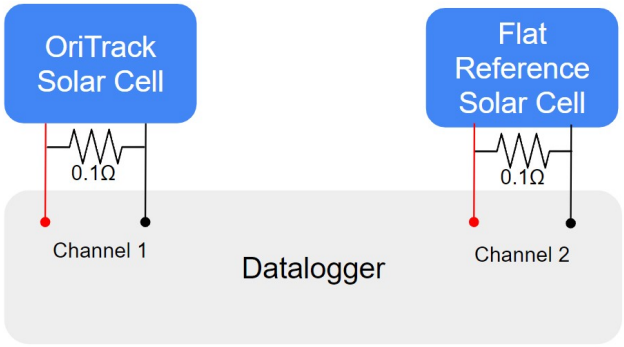

Figure 8. Image of the solar tracking test setup

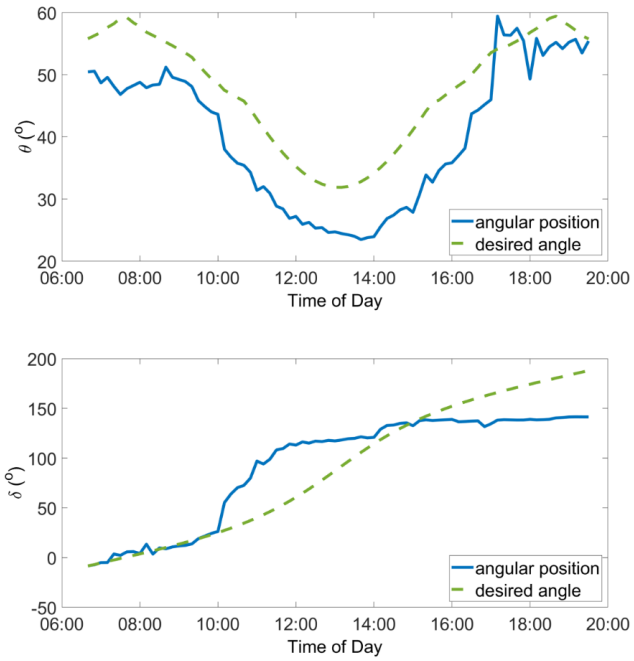

Figure 9. A plot showing the desired and actual solar tracker output angles throughout the experiment

that occlude neighboring trackers. A single OriTrack was tested from sunrise to sunset outdoors on September 8, 2023 in Mountain View California. On that day it produced 23% more energy when accounting for the energy required to operate the system.

While, 23% energy increase is substantial, this number could be even further increased by improving tracking accuracy and adjusting when OriTrack is in a low-power, non-tracking, mode to optimize energy capture. During our experiment, we observed an RMSE of 8.2° for tracking in θ and an RMSE of 29.2° for tracking in δ. Given that the primary cause of these tracking errors is likely the fact that the kinematic model does not account for compliance in the origami structure, stiffening the unhinged parts of the origami structure is an initial step towards improving tracking accuracy. Many other origami structures have been manufactured from fiberglass or carbon fiber and polyimide composites, where the polyimide is sandwiched between either fiberglass or carbon fiber, providing a more rigid structure [20]–[23], [27], [28]. Similarly, we could also stiffen the chipboard structure we have already used here, by doing a fiberglass layup on the unhinged portions of the chipboard. This last option could be particularly promising as it may help keep the cost of an individual OriTrack low. We would also like to better investigate the timing scheme for when OriTrack is actively moving to align itself with the sun and when it is not. Improving this timing scheme in order to ensure that adjustments in angular position outweigh the energetic cost of that movement could also improve energy capture when compared to a flat reference panel.

In addition to stiffening the unhinged parts of the origami structure, we would also like to investigate improving tracking accuracy through different feedback and control modalities. One potential direction is to install an accelerometer mounted to the underside of the solar panel and employ an operational space controller that uses the estimated solar panel angles derived from accelerometer data to control orientation. Another option could be to use an array of light detecting resistors to measure the location of the sun as done in [6], [29]. Using either of these sources of feedback for the controller would likely improve tracking accuracy as it relies less on a kinematic model that does not account for compliance in the structure.

After improving OriTrack's tracking accuracy, we would also like to continuing investigating how much the change in height over the course of a day reduces self-shading in a larger array of solar trackers in different locations and at different times of year. We would also like to investigate how different array layouts produce different energy increases. When investigating an array of OriTracks we would also like to research shared actuation between trackers and the potential energetic and cost benefits of that.

Acknowledgment

This work was funded by the Tapestry project at Google X. We also thank Haden Cory, Marina Dolivo, Michael Lopez, and Joseph Matias for their help fabricating the OriTrack prototype.

References

[1] "Annual 2022 global climate report," *Annual 2022 Global Climate Report — National Centers for Environmental Information (NCEI)*, Jan 2023. [Online]. Available: https://www.ncei.noaa.gov/access/monitoring/monthly-report/global/202213

[2] K. Abbas, M. Z. Qasim, H. Song, M. Murshed, H. Mahmood, and I. Younis, "A review of the global climate change impacts, adaptation, and sustainable mitigation measures," *A review of the global climate change impacts, adaption, and sustainable mitigation measures*, vol. 20, pp. 42 539–52 559, June 2022.

[3] C. O'Neil and H. Dreves, "Building a solar-powered future," Feb 2022. [Online]. Available: https://www.nrel.gov/news/program/2022/building-a-solar-powered-future.html

[4] R. Sharma, "Effect of obliquity of incident light on the performance of silicon solar cells," *Heliyon*, vol. 5, July 2019.

[5] A. Awasthi, A. K. Shukla, M. M. S.R., C. Dondariya, K. Shukla, D. Porwal, and G. Richhariya, "Review on sun tracking technology in solar pv system," *Energy Reports*, vol. 6, pp. 392–405, 2020. [Online]. Available: https://www.sciencedirect.com/science/article/pii/S2352484719304780

[6] F. M. Hoffmann, R. F. Molz, J. V. Kothe, E. O. B. Nara, and L. P. C. Tedesco, "Monthly profile analysis based on a two-axis solar tracker proposal for photovoltaic panels," *Renewable Energy*, vol. 115, pp. 750–759, 2018. [Online]. Available: https://www.sciencedirect.com/science/article/pii/S0960148117308388

[7] A. Amelia, Y. Irwan, I. Safwati, W. Leow, M. Mat, and M. S. A. Rahim, "Technologies of solar tracking systems: A review," *IOP Conference Series: Materials Science and Engineering*, vol. 767, no. 1, p. 012052, feb 2020. [Online]. Available: https://dx.doi.org/10.1088/1757-899X/767/1/012052

[8] H. Fathabadi, "Comparative study between two novel sensorless and sensor based dual-axis solar trackers," *Solar Energy*, vol. 138, pp. 67–76, 2016. [Online]. Available: https://www.sciencedirect.com/science/article/pii/S0038092X16304042

[9] D. Flores-Hernández, S. Palomino-Resendiz, N. Lozada-Castillo, A. Luviano-Juárez, and I. Chairez, "Mechatronic design and implementation of a two axes sun tracking photovoltaic system driven by a robotic sensor," *Mechatronics*, vol. 47, pp. 148–159, 2017. [Online]. Available: https://www.sciencedirect.com/science/article/pii/S0957415817301381

[10] Y. Away and M. Ikhsan, "Dual-axis sun tracker sensor based on tetrahedron geometry," *Automation in Construction*, vol. 73, pp. 175–183, 2017. [Online]. Available: https://www.sciencedirect.com/science/article/pii/S0926580516303156

[11] S. Abdallah and S. Nijmeh, "Two axes sun tracking system with plc control," *Energy Conversion and Management*, vol. 45, no. 11, pp. 1931–1939, 2004. [Online]. Available: https://www.sciencedirect.com/science/article/pii/S0196890403003066

[12] S. Yilmaz, H. Riza Ozcalik, O. Dogmus, F. Dincer, O. Akgol, and M. Karaaslan, "Design of two axes sun tracking controller with analytically solar radiation calculations," *Renewable and Sustainable Energy Reviews*, vol. 43, pp. 997–1005, 2015. [Online]. Available: https://www.sciencedirect.com/science/article/pii/S1364032114010375

[13] L. Barker, M. Neber, and H. Lee, "Design of a low-profile two-axis solar tracker," *Solar Energy*, vol. 97, pp. 569–576, 2013. [Online]. Available: https://www.sciencedirect.com/science/article/pii/S0038092X13003757

[14] Y. Yao, Y. Hu, S. Gao, G. Yang, and J. Du, "A multipurpose dual-axis solar tracker with two tracking strategies," *Renewable Energy*, vol. 72, pp. 88–98, 2014. [Online]. Available: https://www.sciencedirect.com/science/article/pii/S0960148114003887

[15] H. Shang and W. Shen, "Design and implementation of a dual-axis solar tracking system," *Energies*, vol. 16, no. 17, 2023. [Online]. Available: https://www.mdpi.com/1996-1073/16/17/6330

[16] Y. Oner, E. Cetin, H. K. Ozturk, and A. Yilanci, "Design of a new three-degree of freedom spherical motor for photovoltaic-tracking systems," *Renewable Energy*, vol. 34, no. 12, pp. 2751–2756, 2009. [Online]. Available: https://www.sciencedirect.com/science/article/pii/S0960148109001864

[17] A. R. Jensen, I. Sifnaios, S. Furbo, and J. Dragsted, "Self-shading of two-axis tracking solar collectors: Impact of field layout, latitude, and aperture shape," *Solar Energy*, vol. 236, pp. 215–224, 2022. [Online]. Available: https://www.sciencedirect.com/science/article/pii/S0038092X22001207

[18] *AllEarth Solar Tracker*, AllEarth Renewables, iNC, August 2023. [Online]. Available: https://www.allearthrenewables.com/wp-content/uploads/2023/08/AER_SolarTracker_InfoSheet_081023.pdf

[19] L. Al Marjan and S.-C. Huang, "Structure of parallel mechanism combined with waterbomb-base-inspired origami," *Engineering Proceedings*, vol. 38, no. 1, 2023. [Online]. Available: https://www.mdpi.com/2673-4591/38/1/51

[20] F. H. Giraud, S. Joshi, and J. Paik, "Haptigami: A fingertip haptic interface with vibrotactile and 3-dof cutaneous force feedback," *IEEE Transactions on Haptics*, vol. 15, no. 1, pp. 131–141, 2022.

[21] S. Mintchev, M. Salerno, A. Cherpillod, S. Scaduto, and J. Paik, "A portable three-degrees-of-freedom force feedback origami robot for human–robot interactions," *Nature Machine Intelligence*, vol. 1, pp. 584–593, 2019.

[22] M. Salerno, K. Zhang, A. Menciassi, and J. S. Dai, "A novel 4-dof origami grasper with an sma-actuation system for minimally invasive surgery," *IEEE Transactions on Robotics*, vol. 32, no. 3, pp. 484–498, 2016.

[23] M. A. Robertson, O. C. Kara, and J. Paik, "Soft pneumatic actuator-driven origami-inspired modular robotic "pneumagami"," *The International Journal of Robotics Research*, vol. 40, no. 1, pp. 72–85, 2021. [Online]. Available: https://doi.org/10.1177/0278364920909905

[24] H. Gang, Y. Fang, and K. Zhang, "Kinematics and workspace analysis of a novel 3-dof parallel manipulator with virtual symmetric plane," *Journal of Mechanical Engineering Science*, vol. 227, no. 3, pp. 620–629, 2012.

[25] A. M. B. Manuel J. Blanco, Kypros Milidonis, "Updating the psa sun position algorithm," *Solar Energy*, vol. 212, pp. 339 – 341, 2020.

[26] *SunPower C60 Solar Cell Mono Crystalline Silicon*, SunPower Corporation, November 2010, rev. **.

[27] H. McClintock, F. Z. Temel, N. Doshi, J. sung Koh, and R. J. Wood, "The millidelta: A high-bandwidth, high-precision, millimeter-scale delta robot," *Science Robotics*, vol. 3, no. 14, p. eaar3018, 2018. [Online]. Available: https://www.science.org/doi/abs/10.1126/scirobotics.aar3018

[28] R. J. W. Hiroyuki Suzuki, ""origami-inspired miniature manipulator for teleoperated microsurgery"," *Nature Machine Intelligence*, vol. 2, pp. 437–446, 2020.

[29] T. Kaur, S. Mahajan, S. Verma, Priyanka, and J. Gambhir, "Arduino based low cost active dual axis solar tracker," in *2016 IEEE 1st International Conference on Power Electronics, Intelligent Control and Energy Systems (ICPEICES)*, 2016, pp. 1–5.